JOURNAL OF MATERIALS SCIENCE 28 (1993) 4904–4909

Sintering and crystallization of mullite powder prepared by sol–gel processing

D.-Y. JENG*, M. N. RAHAMAN‡
Department of Ceramic Engineering, University of Missouri-Rolla, Rolla, MO 65401, USA

Mullite powder with the stoichiometric composition ($3Al_2O_3.2SiO_2$) was synthesized by a sol–gel process, followed by hypercritical drying with CO_2. Within the limits of detection by X-ray diffraction, the powder was amorphous. Crystallization of the powder commenced at $\approx$1200 °C and was completed after 1 h at 1350 °C. *In situ* X-ray analysis showed no intermediate crystalline phases prior to the onset of mullite crystallization and the pattern of the fully crystallized powder was almost identical to that of stoichiometric mullite. The synthesized powder was compacted and sintered to nearly theoretical density below $\approx$1250 °C. The microstructure of the sintered sample consisted of nearly equiaxial grains with an average size of $\approx$0.2 μm. The effect of heating rate (1–15 °C min^{-1}) on the sintering of the compacted powder was investigated. The sintering rate increased with increasing heating rate, and the maximum in the sintering curve shifted to higher temperatures. The sintering kinetics below $\approx$1150 °C can be described by available models for viscous sintering.

1. Introduction

Experimental studies [1–4] have demonstrated that amorphous (or glass) matrices are easier to densify around a rigid inclusion phase (in the form of particles, whiskers or fibres) compared to polcrystalline matrices. Densification prior to crystallization (referred to as a "glass-ceramic route") is therefore expected to be particularly important for achieving high density composites by conventional, pressureless sintering. However, after sintering, it will be necessary to control the nucleation and growth of the crystalline phase to obtain the required microstructure.

The purpose of the research reported in this paper was to synthesize an "amorphous" mullite powder with the stoichiometric composition ($3Al_2O_3.2SiO_2$) and to investigate its sintering and crystallization. (The term "amorphous" is used here to signify the absence of a well-defined crystal pattern as revealed by X-ray diffraction.) The powder was synthesized by a sol–gel technique. In two subsequent papers [5, 6], the use of the synthesized powder as the matrix phase for composites with high sinterability will be reported.

Mullite was chosen for this investigation because it is a useful model material that has been studied extensively. It is also an important material for many technological applications (e.g. heat engines, electronic substrates and microwave dielectrics). A number of techniques have been used to synthesize mullite powder [7–11]. Among these, the sol–gel process offers the advantages of good mixing of the starting materials and good chemical homogeneity of the product. Mullite gel can be synthesized from a number of different starting materials, including (a) a mixture of two alkoxides [12, 13], usually tetraethylorthosilicate (TEOS) and aluminum *s*-butoxide, (b) a mixture of an inorganic salt and an alkoxide [14], usually aluminium nitrate and TEOS, and (c) two sols [14], usually silica and bohemite. In the present research, two alkoxides (TEOS and aluminium *s*-butoxide) were used as the starting materials.

The initial step in the formation of mullite gel starting from two alkoxides is the addition of water to promote hydrolysis, condensation and gelation of the mixture. By appropriate control of the concentration of the reactants and the pH of the solution, either linear polymers or weakly cross-linked polymers can be formed [15]. After the gel is formed, drying is accomplished by removal of liquid in the pores. The widely used, conventional method of drying involves exposure to the atmosphere or vacuum at room temperature or below $\approx$100 °C. Evaporation of liquid and liquid redistribution lead to capillary stresses [16, 17] which, in turn, cause shrinkage and an increase in the effective viscosity of the gel. If the stresses are large enough, they can cause cracking in the gel.

A less widely used method of drying involves hypercritical extraction [13, 18–21] of the liquid in the gel structure. Due to the absence of liquid–vapour interfaces, no capillary stresses arise to cause network collapse. Drying shrinkages are therefore small and the gel has a relatively low viscosity compared to the conventionally-dried gel. From the point of view of forming a powder, the hypercritical drying process has a distinct advantage in that the dried gel can be

* *Present address*: Department of Materials Science and Engineering, University of California, Los Angeles, CA 90024, USA.
‡ Author to whom correspondence should be addressed.

0022–2461

ground into a powder much more easily compared with the conventionally-dried gel.

After drying, the gel may be sintered to produce a dense material. Sintering of amorphous or glassy materials has been modelled by Scherer [22]. According to Scherer, the sintering rate, ε, can be expressed by an equation of the form

$$\varepsilon = A\gamma_{sv} n^{1/3}/\eta \quad (1)$$

where A is a constant, γ_{sv} is the solid–vapour surface energy, n is the number of pores per unit volume, and η is the viscosity of the solid phase. The benefits of a low viscosity matrix for sintering is apparent from Equation 1.

In the present paper, the synthesis of mullite powder by sol–gel processing followed by hypercritical drying is described. The sintering, crystallization and microstructure development of the compacted powder at constant rates of heating were investigated.

2. Experimental procedure

2.1. Preparation of mullite powder

Mullite gel with the stoichiometric composition ($3Al_2O_3.2SiO_2$) was prepared by the hydrolysis, condensation and gelation of aluminium *s*-butoxide and tetraethyl orthosilicate (TEOS). (Both chemicals were Reagent Grade, and were obtained from Alfa Chemicals, Danvers, MA, USA). A solution of aluminium butoxide (molar ratio of H_2O: butoxide = 50:1) was hydrolysed at 90 °C for 1 h and then peptized by adding HNO_3 (molar ratio of butoxide:acid = 1:0.1). After the peptized mixture became transparent, the required amount of TEOS (dissolved in ethanol) was added to the mixture. Gelation occured in minutes under vigorous stirring at 75 °C. The gelled material was aged and soaked in ethanol several times (to replace the liquid in the pores with ethanol) prior to drying by hypercritical extraction with CO_2.

In the drying process, the wet gel was first placed in an autoclave which was then filled with ethanol. The ethanol was then displaced by flowing liquid CO_2 into the autoclave at a pressure of 800 psi for 8–10 h. When no trace of ethanol could be detected in the mixture flowing through the outlet, the autoclave was cooled to 8 °C while maintaining the pressure at 800 psi. The inlet and outlet valves were then closed and the temperature of the autoclave was raised to 40 °C while the pressure was maintained at 1200 psi. These hypercritical conditions for the CO_2 were maintained for 4 h, after which the pressure was released slowly to bring the system to ambient pressure. The temperature was then reduced to room temperature. At this point, a dry low-density gel with a solids content of < 10 vol % was obtained.

The gel was heated to 150 °C for 24 h to remove any traces of liquid and then heated at 600 °C for 4 h to burn off organics present from the sol–gel process. The pyrolysed gel was then ground lightly in a plastic mortar and pestle to produce a powder. Compaction of the powder was performed by pressing uniaxially in a die at ≈10 MPa to form cylindrical pellets (12 mm in diameter by 6 mm) which were further pressed isostatically at ≈300 MPa to produce samples with a green relative density of 0.45 ± 0.01.

2.2. Sintering of the compacted powder

The powder compacts were sintered in air in a 1600 °C dilatometer (Theta Industries, Inc., Port Washington, NY, USA) that allowed continuous monitoring of the shrinkage. Sintering experiments were performed initially at a constant heating rate of 4 °C min^{-1} to 1350 °C, followed by a 1 h hold at this temperature. Further experiments were performed to investigate the effect of heating rate on the sintering of the compacted mullite powder. In these experiments, the samples were sintered under four imposed heating rates of 1, 5, 10 and 15 °C min^{-1} to 1500 °C. Lower heating rates were very time consuming, while higher heating rates could not be readily obtained with the dilatometer.

The mass and dimensions of the compacts were measured before and after they were sintered. The density at any temperature (or time) was calculated from the initial density and the measured shrinkage. The final densities of the sintered samples were also measured using Archimedes' principle. The theoretical density of stoichiometric mullite was assumed to be 3.17 g cm^{-3}.

2.3. Characterization of the samples

Differential thermal analysis (DTA) and thermogravimetric analysis (TGA) were used to study the changes occurring in the synthesized powder during calcination. The samples were heated at a constant rate of 10 °C min^{-1} to 1500 °C.

The microstructure of the sintered samples was observed using scanning electron microscopy of both fracture surfaces and polished and thermally etched surfaces. Thermal etching was performed for 2 h at 1400 °C in air. Grain size and grain morphology of the sintered material were observed using transmission electron microscopy (TEM). Observations were accomplished by both bright field (BF) and electron diffraction (ED) techniques.

The phase composition of the synthesized powder and of the sintered material was determined by X-ray diffraction (XRD) in a diffractometer equipped with a hot stage. CuK_α radiation was used in the 2θ range of 20–60° at a scanning rate of 2° 2θ per minute. For analysis of the sintered samples, the compact was ground to a fine powder in an agate mortar and pestle. The crystallization of the mullite powder on heating was determined by *in situ*, hot stage XRD. In these experiments, the powder was placed on a platinum strip which was heated in air at a rate of 5 °C min^{-1} to 1350 °C. The diffraction pattern was recorded at 100 °C intervals between 900 and 1300 °C.

3. Results

3.1. Constant heating rate sintering

Fig. 1 shows the axial shrinkage, $\Delta L/L_0$, versus temperature, T, for the compacted mullite powder (green density 0.45) during sintering at four different heating

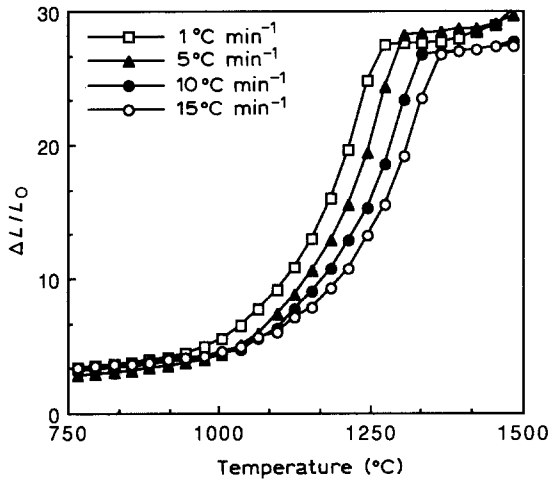

Figure 1 Axial shrinkage versus temperature for the synthesized mullite powder compacted to a relative density of 0.45 and sintered at 1, 5, 10 and 15 °C min^{-1} to 1500 °C.

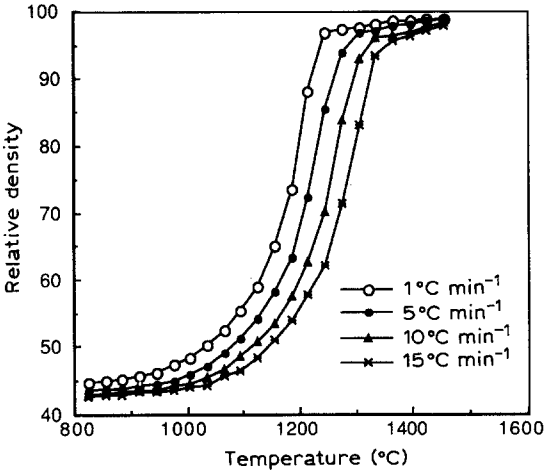

Figure 2 Relative density versus temperature for the samples described in Fig. 1.

rates, α, of 1, 5, 10 and 15 °C min^{-1}. (L_0 = initial sample length, and $\Delta L = L - L_0$, where L is the instantaneous sample length). Each curve is the average of two runs under the same conditions and is reproducible to < 0.1 %. The curves have somewhat similar shapes but are shifted to higher temperatures with increasing α. For the sample sintered at 5 °C min^{-1}, shrinkage commenced at ≈900 °C and was almost completed at ≈1250 °C; the shrinkage rate was highest, however, between ≈1100 and 1200 °C. The sintered density, measured by Archimedes' principle, was in excellent agreement with a value of 0.98 obtained from measurements of the sample mass and dimensions. The nearly theoretical density obtained at ≈1250 °C is comparable to that of mullite prepared by a similar technique [13] and is slightly higher than those for mullite gels prepared by conventional drying [14] (i.e. exposure to the atmosphere). The final density is also much higher than those reported by others for mullite prepared by various, more conventional techniques [11].

The relative density, ρ, of the samples at any temperature was calculated from the data of Fig. 1 according to the relation

$$\rho = \rho_0/(1 - \Delta L/L_0)^3 \quad (2)$$

where ρ_0 is the initial relative density. The results are shown in Fig. 2. The temperature at which densification was almost completed increased from ≈1200 °C for α = 1 °C min^{-1} to ≈1350 °C for α = 15 °C min^{-1}. The volumetric densification rate, defined as $(1/\rho)\, d\rho/dt$, was calculated by fitting smooth curves to the data of Fig. 2 and differentiating. Fig. 3 shows that with increasing α, the densification rate at any temperature increases and the maximum in the curve is shifted to higher temperatures.

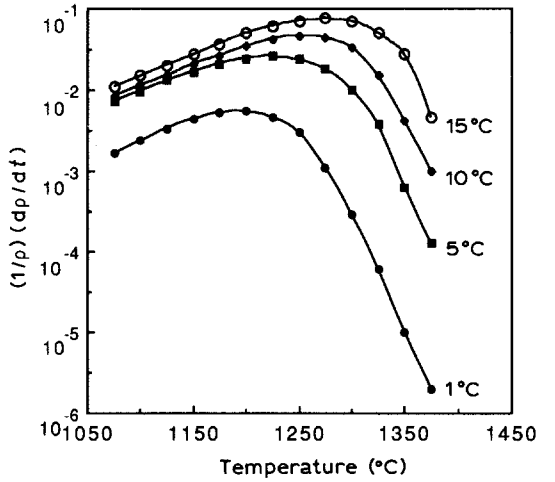

Figure 3 Densification rate versus temperature calculated from the data of Fig. 2.

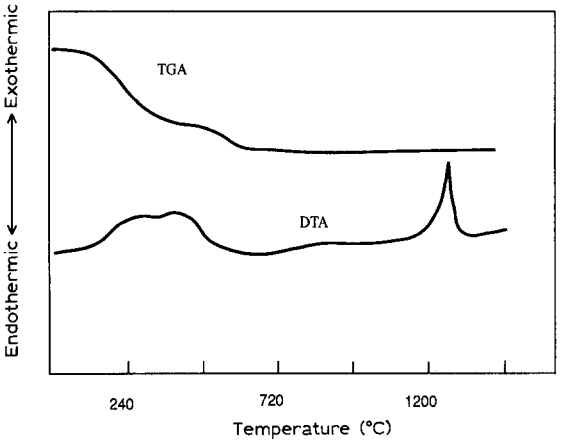

Figure 4 Differential thermal analysis (DTA) and thermogravimetric analysis (TGA) curves for the synthesized mullite powder heated at 10 °C min^{-1} to 1500 °C.

3.2. Crystallization of the mullite powder

DTA and TGA analysis of the amorphous mullite powder was performed at a constant heating rate of 10 °C min^{-1} and the results are shown in Fig. 4. The powder was dried overnight at ≈100 °C and stored in a desiccator prior to the analysis. The DTA curve shows a broad exotherm between ≈200 and 500 °C, which is attributed to the removal of organics and hydroxyl groups. The TGA curve shows a corresponding weight loss within this temperature region. Above ≈500 °C, there is almost no further weight loss. The total weight loss after heating to 1500 °C is

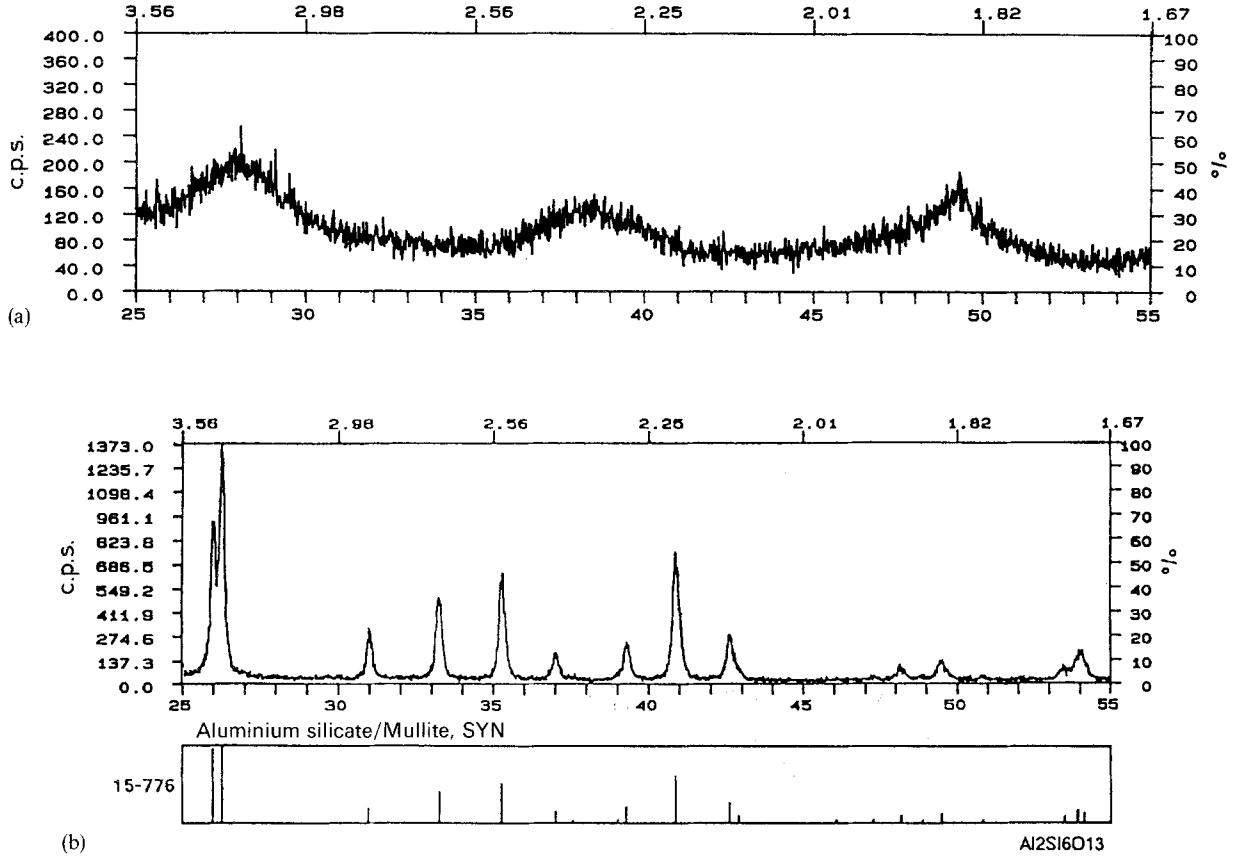

Figure 5 X-ray diffraction patterns of (a) the synthesized mullite powder and (b) the crystallized mullite which was heated to 1350 °C for 1 h. (The abscissa is in units of degrees 2θ.)

≈13 %. The sharp exotherm in the DTA curve at ≈1250 °C corresponds to the crystallization of the mullite powder. It is interesting to note that the DTA curve shows no evidence of crystallization of other phases prior to the crystallization peak at ≈1250 °C.

X-ray analysis of the synthesized mullite powder after drying overnight at ≈100 °C does not reveal any well-developed crystalline peaks [Fig. 5(a)]. The fully crystallized powder produced by heating at 1350 °C for 1 h shows well-defined peaks which are almost identical to those of stoichiometric mullite [Fig. 5(b)].

Fig. 6 shows the crystallization behaviour of the synthesized mullite powder as determined by *in situ* hot-stage X-ray diffraction. The peak at ≈40 °2θ is due to the sample holder. It should be pointed out that due to the small amount of powder that can be placed on the sample holder and the resulting low density of the sample, the diffraction peaks were not as sharp and well-defined as for a more densely packed sample. Crystallization commenced at ≈1100 °C and became quite noticeable at 1200 °C, which is close to the crystallization temperature observed by DTA. Within the detection limits of the *in situ* X-ray analysis, no intermediate phases were observed prior to the crystallization of mullite.

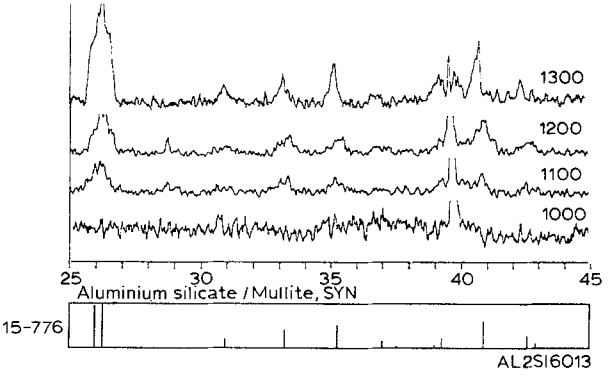

Figure 6 In situ, hot stage X-ray diffraction pattern of the synthesized mullite powder heated at 5 °C min^{-1} to the temperatures shown in °C. (The abscissa is in units of degrees 2θ.)

3.3. Microstructure development

Fig. 7 shows SEM micrographs of (a) the fracture surface and (b) the polished and thermally etched surface of a mullite powder compact (initial relative density = 0.45) that was sintered at 4 °C min^{-1} to 1350 °C. The measured density of the sintered compact was 0.98. The micrograph of the polished and etched surface shows some evidence of a very fine-grained microstructure.

Transmission electron microscopy was used to achieve better resolution of the sintered microstructure. Bright field TEM (Fig. 8) shows a nearly equiaxed microstructure with an average grain size of ≈0.2 μm. Within the resolution limits of the instrument, no glassy phases were detected in the grain boundaries. Selected area diffraction confirmed the crystalline nature of the sintered sample.

4. Discussion

The mullite powder synthesized in this work by

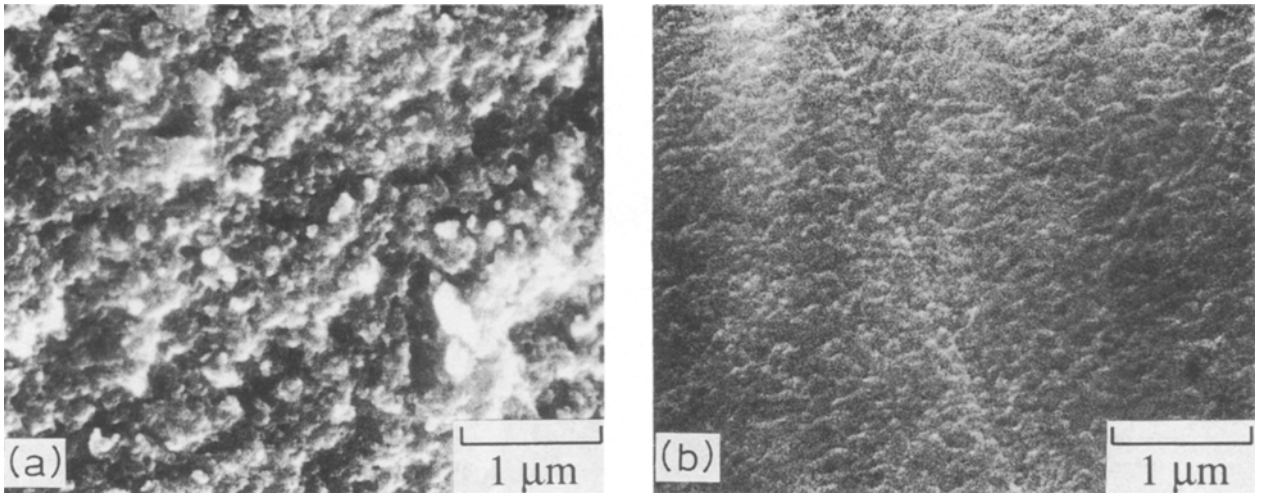

Figure 7 Scanning electron micrograph of (a) the fracture surface and (b) the polished and thermally etched surface of a sample sintered at 4 °C min^{-1} to 1350 °C.

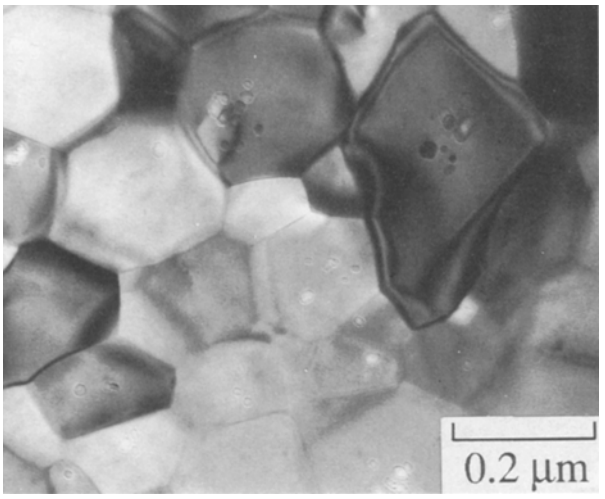

Figure 8 Bright field transmission electron micrograph of a mullite sample sintered for 1 h at 1350 °C.

sol–gel processing followed by hypercritical drying shows a number of desirable sintering characteristics. The compacted powder sintered to nearly theoretical density below ≈1250 °C, which is nearly 400 °C lower than the sintering temperature required for the formation of dense stoichiometric mullite from mixed powders of Al_2O_3 and SiO_2. The absence of intermediate crystallization prior to the main mullite crystallization temperature of ≈1200 °C indicates that the process is much less complex compared to the crystallization phenomena observed in samples prepared from mixed powders [23, 24]. The absence of intermediate phases (which is desirable) may be due to the good chemical uniformity of the mullite powder synthesized in this work. This chemical uniformity may also be an important factor in the formation of the nearly equiaxial, fine-grained microstructure during sintering (Fig. 8). Although no studies were performed on the sintered mullite, the very fine-grained microstructure may be expected to give rise to limited superplasticity during deformation at elevated temperatures.

The sintering and crystallization studies (Figs 2, 4 and 6) show that most of the densification of the compacted mullite powder occurred prior to crystallization. This is expected to be an important factor for the formation of high density composites by conventional sintering since, as pointed out earlier, an amorphous matrix sinters more easily around a reinforcement phase compared to a polycrystalline matrix. The use of the synthesized mullite powder for the matrix phase of composites is described in subsequent papers [5, 6].

Since most of the densification of the compacted mullite powder occurred prior to crystallization, it would be expected that the dominant sintering mechanism would be viscous flow. It would be interesting to see whether the theories of viscous sintering can account for the measured sintering kinetics. While Scherer's model [22] for viscous sintering might be more appropriate to the present work, it has been shown that the predictions of the model do not differ significantly from those of the somewhat simpler model of Mackenzie and Shuttleworth [25]. In the present discussion, the Mackenzie and Shuttleworth model will therefore be used. The model predicts that the densification rate, defined as $(1/\rho)\,d\rho/dt$, is given by

$$(1/\rho)d\rho/dt = (\gamma_{sv}/\eta)\{4\pi n\rho/[3(1-\rho)]\}^{1/3} \quad (3)$$

where ρ is the density, t is the time, and the other terms have been defined in Equation 1. In constant heating rate sintering, the temperature is given by

$$T = T_0 + \alpha t, \quad (4)$$

where T_0 is the initial temperature. Assuming that η is given by

$$\eta = \eta_0 \exp[\Delta G/(RT)] \quad (5)$$

where ΔG is the activation energy for viscous flow and R is the gas constant, then Equation 3 can be written

$$\frac{1}{3}\int_{\rho_o}^{\rho} \frac{(1-\rho)^{\frac{1}{3}}}{\rho^{\frac{4}{3}}}\,d\rho = F(\rho) = \frac{\gamma_{sv}K}{\alpha\eta_0}\int_{T_0}^{T} \exp\left(\frac{-\Delta G}{RT}\right)dT \quad (6)$$

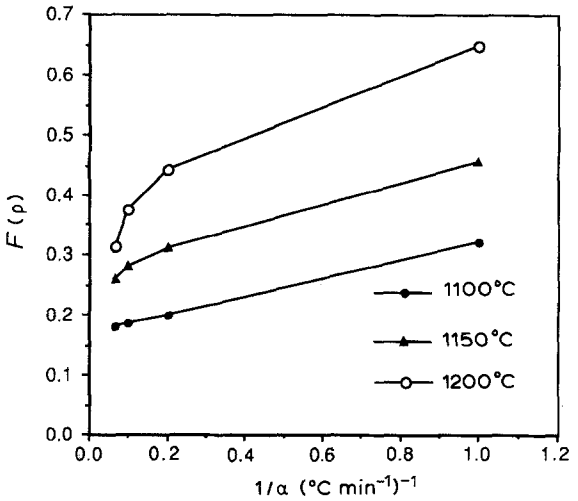

Figure 9 Data for the density function, $F(\rho)$, in Equation 6 versus the inverse of the heating rate at fixed temperatures of 1100, 1150 and 1200 °C.

where $K = (4\pi n/3)^{1/3}$. According to Equation 6, a plot of $F(\rho)$ versus $1/\alpha$ should yield a straight line. This is indeed found to be so for temperatures up to ≈ 1100 °C (Fig. 9). Deviations from the straight line above this temperature may be due to the onset of crystallization. When crystallization occurs, then Equation 5 will no longer be valid.

5. Conclusions

Mullite powder, synthesized by a sol–gel technique followed by hypercritical drying with CO_2, was compacted and sintered to nearly theoretical density below ≈ 1250 °C. This density is somewhat higher than those reported for mullite gels prepared by a similar sol–gel technique followed by conventional drying, and is considerably higher than those for mullite prepared from mixed powders.

Crystallization of the synthesized powder commenced at ≈ 1100–1200 °C and was completed after 1 h at 1350 °C. Within the detection limits of the equipment, the X-ray diffraction pattern of the fully crystallized mullite was almost identical to that of stoichiometric mullite and no intermediate crystalline phases were detected prior to the onset of mullite crystallization.

Bright field transmission electron microscopy showed that the sintered, fully dense mullite consisted of nearly equiaxed grains with an average size of ≈ 0.2 μm.

The sintering kinetics prior to the crystallization of the sample (i.e. below ≈ 1100 °C) can be explained by existing models for viscous sintering.

References

1. L. C. DE JONGHE, M. N. RAHAMAN and C. H. HSUEH, *Acta Metall.* **34** (1986) 1467.
2. M. N. RAHAMAN and L. C. DE JONGHE, *J. Amer. Ceram. Soc.* **70** (1987) C-348.
3. R. K. BORDIA and R. RAJ, *ibid.* **71** (1988) 302.
4. W. H. TUAN, E. GILBART and R. J. BROOK, *J. Mater. Sci.* **24** (1989) 1062.
5. M. N. RAHAMAN and D.-Y. JENG, *J. Mater. Sci.*, submitted.
6. D.-Y. JENG and M. N. RAHAMAN, *J. Amer. Ceram. Soc.*, in press.
7. K. S. MASDIYASNI and L. M. BROWN, *ibid.* **55** (1972) 548.
8. B. L. METCALF and J. H. SANT, *Trans. J. Brit. Ceram. Soc.* **74** (1975) 193.
9. H. YAMADA and S. KIMURA, *J. Ceram. Soc. Jpn* **70** (1972) 63.
10. B. B. GHATE, D. P. H. HASSELMAN and R. M. SPRIGGS, *Amer. Ceram. Soc. Bull.* **52** (1973) 670.
11. S. KANZAKI, H. TABATA, T. KUMAZAWA and S. OHTA, *J. Amer. Ceram. Soc.* **68** (1985) C-6.
12. B. E. YOLDAS, *J. Mater. Sci.* **12** (1977) 1203.
13. M. N. RAHAMAN, L. C. DE JONGHE, S. L. SHINDE and P. H. TEWARI, *J. Amer. Ceram. Soc.* **71** (1988) C-338.
14. S. KOMARNENI, Y. SUWA and R. ROY, *ibid.* **69** (1986) C-155.
15. C. J. BRINKER and G. W. SCHERER, *J. Non-Cryst. Solids* **70** (1985) 301.
16. J. ZARZYCKI, M. PRASSAS and J. PHALIPPOU, *J. Mater. Sci.* **17** (1982) 3371.
17. G. W. SCHERER, *J. Non-cryst. Solids* **87** (1986) 199.
18. S. S. KISTLER, *J. Phys. Chem.* **36** (1932) 52.
19. G. A. NICHOLSON and S. J. TEICHNER, *Bull. Soc. Chim. Fr.* **58** (1968) 1906.
20. S. P. MUKHERJEE and J. C. DEBSIKDAR, *Amer. Ceram. Soc. Bull.* **62** (1983) 413.
21. P. H. TEWARI, A. J. HUNT and K. D. LOFFTUS, *Mater. Lett.* **3** (1985) 363.
22. G. W. SCHERER, *J. Amer. Ceram. Soc.* **60** (1977) 236.
23. I. A. AKSAY and J. A. PASK, *ibid.* **58** (1975) 507.
24. J. A. PASK, *Ceram. Int.* **9** (1983) 107.
25. J. K. MACKENZIE and R. SHUTTLEWORTH, *Proc. Phys. Soc. Lond.* **62** (1949) 838.

Received 26 February
and accepted 10 December 1992